IEEE Access
Multidisciplinary | Rapid Review | Open Access Journal

Received September 19, 2021, accepted September 24, 2021, date of publication September 27, 2021,
date of current version October 11, 2021.

Digital Object Identifier 10.1109/ACCESS.2021.3115909

Design of an Adaptive Fuzzy Observer-Based Fault Tolerant Controller for Pneumatic Active Suspension With Displacement Constraint

CONG MINH HO AND KYOUNG KWAN AHN, (Senior Member, IEEE)
School of Mechanical and Automotive Engineering, University of Ulsan, Ulsan 44610, South Korea

Corresponding author: Kyoung Kwan Ahn (kkahn@ulsan.ac.kr)

This work was supported by the Basic Science Program through the National Research Foundation of Korea (NRF) funded by the Ministry of Science and ICT, South Korea, under Grant NRF-2020R1A2B5B03001480.

ABSTRACT This paper proposes an adaptive fuzzy observer based fault tolerant controller for a pneumatic active suspension system considering unknown parameters, actuator failures, and displacement constraints. A pneumatic spring is used for a quarter car model to enhance the vibration attenuation performance. Since the pneumatic system contains uncertain nonlinearities, fuzzy logic systems are utilized to approximate unknown nonlinear functions of unmodeled dynamics and various masses of passengers. Besides, a nonlinear disturbance observer is proposed to estimate the effects of the actuator failures, approximation errors, and external disturbances. By utilizing the disturbance estimation and fuzzy approximation techniques, an adaptive fault tolerant control (FTC) is designed to enhance the output performance of the vehicle suspension. Meanwhile, the command filtered scheme is introduced to solve the explosion of complexity problem in the traditional backstepping approach by avoiding virtual controller derivatives. In contrast to previous results, the proposed control can handle the fault tolerant problem and ensure the tracking error of vertical displacement converges into a small-predefined boundary by introducing the prescribed performance function. Moreover, the stability of the closed-loop system is analyzed according to the Lyapunov theory. Finally, comparative simulation examples and experimental studies are performed on the active pneumatic suspension test bench to verify the feasibility of the proposed scheme.

INDEX TERMS Active suspension systems (ASSs), nonlinear disturbance observer (NDOB), prescribed performance function (PPF), fuzzy logic systems (FLSs), command filtered control (CFC).

I. INTRODUCTION

With the development of the automotive industry, the suspension system is the most important component of the vehicle chassis, which can improve passenger comfort and driving safety [1]. Therefore, the active suspension designs have attracted significant attention during the past decades by adopting a wide variety of actuators, involving electromagnetic [2] and hydraulic actuators [3]. To better vibration isolation, pneumatic actuators are extensively considered and applied both in automobile research and manufacturing due to high reliability and ease of installation features [4]. By regulating the inlet and exhaust airflow between the air bellow and the pressure source, the ride height and stiffness coefficient of the suspension system can be controlled simultaneously to enhance ride comfort [5]. However, the dynamic model of air spring contains lumped parametric uncertainties due to the thermodynamic characteristics while the pneumatic stiffness depends on the bellow rubber's behavior under external force [6]. Besides, there are still several challenges in designing the controller for pneumatic suspension as it requires controlling the air spring and proportional pressure valve simultaneously. In particular, it is very important to ensure the chassis stability under the presence of unknown masses of passengers and various road conditions.

To further enhance the suspension performance, many advanced controllers have been investigated to handle various problems, including adaptive control [7], optimal control [8], sliding mode control [9], [10], and backstepping control [11]. Nazemian and Masih-Tehrani [12] developed an

The associate editor coordinating the review of this manuscript and approving it for publication was Giovanni Pau.

optimized controller to maximize the dynamic performance and reduce the energy assumption of the pneumatic suspension. Some adaptive sliding mode controllers were proposed to address the unknown dynamics of the pneumatic suspension [13], [14]. Rui [15] designed an adaptive sliding mode control considering the nonlinear dynamical characteristic of the pneumatic system. To improve the ride height motion for pneumatic active suspension under the presence of parametric uncertainties and unmodeled dynamics, the backstepping technique has been applied in [16], [17]. Besides, the problem of hard constraints for ASSs was solved by the backstepping control schemes in [18]. Zhang *et al.* [19] designed the adaptive backstepping control to enhance the ride comfort by regulating the chassis displacement. To guarantee the tracking error and convergence rate of the system states under the maximum overshoot, a new control scheme combining PPF was introduced to improve the output constraints [20], [21]. However, in most previous works, the suspension systems were assumed that accurate mathematical models were established even though parametric uncertainties or external disturbances in physical systems always exist, which make adverse effects on the control objectives.

Since the neural networks control and fuzzy logic systems technique have proved the ability to approximate unknown functions [22], several intelligent controllers using these approximation methods have been developed for the ASSs [23], [24]. In particular, these intelligent control methods can be well combined with backstepping to effectively improve the control performance of suspension systems [25], [26]. Because the ASSs contain uncertain parameters, neural networks are employed to estimate these unknown functions [27]. Li *et al.* [28] proposed an adaptive event-triggered fuzzy controller which considered the nonlinear uncertainties for the ASSs. To reject the disturbances caused by actuator saturation, a disturbance observer based Takagi-Sugeno fuzzy control was designed for an active seat suspension to guarantee passenger comfort by Ning *et al.* [29]. Although these aforementioned approaches can satisfy the requirement of suspension, the explosion of complexity problem induced by repetitive virtual controller derivatives can limit the scope of the traditional backstepping application [30], [31]. Fortunately, dynamic surface control can solve this limitation by introducing a first-order filter to estimate these derivatives. However, the errors caused by the filters are not considered in this technique, which could reduce the control performance definitely [3]. As an alternative, a command filtered control can solve this problem [32]. By adopting error compensation mechanisms, CFC can diminish the errors of the command filters to improve the control efficiency [33]. Nonetheless, only a few studies applied CFC and FLS for the pneumatic ASSs.

On the other hand, most previous results assumed that the suspension systems were in fault-free operating conditions and that ideal actuator behavior was implemented for the control designs [34], [35]. However, various unpredictable actuator failures often occur in the control system, which may degrade the output suspension performance and even lead to controller instability [36], [37]. To enhance the control efficiency and guarantee system reliability, the issue of fault tolerant should be investigated for the suspension control designs [38]. Hence, some researchers have proposed many adaptive controllers to solve the problems of sensor and actuator failures for many years [39]–[41]. A fault tolerant scheme is an effective approach to solve the problem of actuator failures and it can ensure the desired performance by combing the proper controller with an approximation technique [42], [43]. Jing and Yang [44] investigated an adaptive fuzzy observer-based fault tolerant tracking control for uncertain nonlinear systems which considered the unmatched external disturbances and actuator failure problems. Wang *et al.* [45] suggested the output feedback fault tolerant control to improve the passenger comfort for the ASSs. Nonetheless, these studies investigated adaptive fault tolerant schemes based on traditional backstepping technology, which cannot accommodate the explosion of complexity problem [46], [47]. Furthermore, there are a few adaptive fault tolerant controllers based on CFC technique for pneumatic ASSs with non-ideal actuator and parametric uncertainties, which make the motivation for this research.

Basing on the above discussions, we investigate an adaptive fault tolerant tracking control for the pneumatic ASSs using the fuzzy nonlinear disturbance observer method in this paper. Because the active suspension with the pneumatic actuator contains unknown parameters and nonlinearities, it is not easy to establish an accurate system model. Moreover, the suspension system is affected by external disturbances due to various masses of passengers. Although some advanced controllers have been applied to handle these unknown parameters, the actuator failure problems of air spring still need more attention to enhance the control performance. Thus, the FLSs are applied to approximate these unknown nonlinear functions and improve the requirement of modeling precision. Then, a nonlinear disturbance observer is introduced by constructing FLSs to better deal with the actuator failures, approximation errors, and external disturbances. Due to the limitations of the mechanical design, the control objectives of ride comfort and suspension deflection for the ASSs conflict with each other [48]. Besides, some studies can guarantee the control objectives and keep the vertical displacement does not violate the output constraint, but they did not consider the actuator failures. Unlike some previous fault tolerant controllers, the proposed control not only guarantees the tracking performance by introducing the PPF constraint but also eliminates the explosion of complexity problem with the CFC technique. The tracking errors can be guaranteed to converge a small neighborhood of the origin, and the stability of the closed-loop system is proven according to the Lyapunov theory. The main contributions of this paper are summarized as follows

1. A quarter car model is designed with a pneumatic spring to investigate the behavior of the actual suspension system.

2. An adaptive fuzzy observer-based fault tolerant control is designed for the pneumatic suspension system which considers unknown parameters and actuator failures.

3. CFC combined with PPF can solve the explosion of complexity problem in the traditional backstepping technique and guarantee the tracking error of sprung mass displacement does not violate the constraint boundaries.

The rest of this article is arranged as follows. The problem formulation and fault description are displayed in Section II. The design of an adaptive fuzzy observer-based fault tolerant scheme and system stability analysis are shown in Section III. Furthermore, Section IV verifies the efficiency of the developed scheme by the simulation results while the experimental studies are executed by Section V. Finally, some conclusions were given in Section VI.

II. PROBLEM FORMULATION AND PRELIMINARIES

A. PNEUMATIC QUARTER CAR SUSPENSION MODEL

The active suspension using a pneumatic spring is shown in Fig. 1. The total weight of the passengers and chassis is denoted by the sprung mass m_s while the assembly of the vehicle wheel is represented by the unsprung mass m_{us}. The sprung mass and unsprung mass positions are performed by z_s and z_{us}, respectively. The external disturbance caused by the road profile z_r will generate continuous excitations to the passengers. To get ride comfort, active suspension systems are employed to disperse this vibration. The mechanical equations of the quarter car model can be obtained in the form

$$\begin{aligned} &m_s\ddot{z}_s+F_{sp}(z_s, z_{us}, t)+F_{dp}(\dot{z}_s, \dot{z}_{us}, t)-F_p = 0\\ &m_{us}\ddot{z}_{us}-F_{sp}(z_s, z_{us}, t)-F_{dp}(\dot{z}_s, \dot{z}_{us}, t)\\ &\quad +F_{st}(z_{us}, z_r, t)+F_{dt}(\dot{z}_{us}, \dot{z}_r, t)+F_p = 0 \end{aligned} \tag{1}$$

These forces are generated by the stiffness and damping of mechanical structure and pneumatic spring actuator, which can be calculated by: $F_{sp}(z_s, z_u, t) = (k_s+k_p)(z_s-z_{us})$, $F_{dp}(\dot{z}_s, \dot{z}_{us}, t) = c_d(\dot{z}_s-\dot{z}_{us})$, $F_{st}(z_{us}, z_r, t) = k_{st}(z_{us}-z_r)$, $F_{dt}(\dot{z}_{us}, \dot{z}_r, t) = c_{dt}(\dot{z}_{us}-\dot{z}_r)$, in which k_s, c_d denote the stiffness and damping coefficient of active suspension; k_{st}, c_{dt} are the stiffness and damping coefficient of the tire, and k_p represents the stiffness coefficient of pneumatic spring.

To describe the road holding condition, the expression for the tire force can be given by [49]

$$F_t = \begin{cases} F_{st}+F_{dt} & \text{if } F_{st}+F_{dt} < (m_s+m_{us})\, g \\ 0 & \text{if } F_{st}+F_{dt} \geq (m_s+m_{us})\, g \end{cases} \tag{2}$$

where g is the acceleration of gravity.

Determine the system state variables as: $x_1 = z_s$, $x_2 = \dot{z}_s$, $x_3 = z_{us}$, $x_4 = \dot{z}_{us}$, we can obtain the state space form of the active suspension system as follows

$$\begin{aligned} \dot{x}_1 &= x_2\\ \dot{x}_2 &= \frac{1}{m_s}\left[-\left(k_s+k_p\right)(x_1-x_3)-c_d\,(x_2-x_4)+F_p\right]\\ \dot{x}_3 &= x_4 \end{aligned}$$

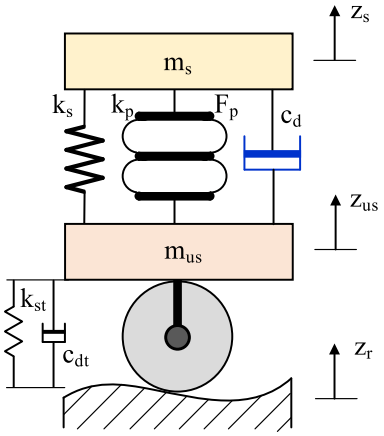

FIGURE 1. Pneumatic active suspension model.

$$\dot{x}_4 = \frac{1}{m_{us}}\left[\begin{array}{l} -k_{st}\,(x_3-z_r)-c_{dt}\,(x_4-\dot{z}_r)\\ +\left(k_s+k_p\right)(x_1-x_3)+c_d\,(x_2-x_4)-F_p \end{array}\right] \tag{3}$$

Compared with the other suspension systems, a pneumatic spring is used to achieve the suspension modulation and the active force can be obtained by the following equation

$$F_p = A_{as}P_{as} \tag{4}$$

where P_{as} denotes the internal pressure and A_{as} is the working area of the pneumatic spring.

To archive the suspension performance, the control design is proposed to regulate the volume of airflow through the pneumatic spring. Thus, the thermodynamic theory is applied to describe the dynamic model of pneumatic spring [13]

$$\dot{P}_{as} = \frac{\kappa RT}{V_{as}}\left(s_0 q_{as}-\frac{P_{as}A_{as}\,(x_2-x_4)}{RT}\right) \tag{5}$$

where R denotes the perfect gas constant, κ is the polytropic index, T represents the air temperature, q_{as} is the area-normalized mass flow rate, and s_0 is the orifice open area of the proportional pressure valve.

The working volume of air bellow V_{as} depends on the relative position between the unsprung mass and sprung mass

$$V_{as} = A_{as}\,(z_{as0}+x_1-x_3) \tag{6}$$

where z_{as0} denotes the initial stroke of the pneumatic spring.

Assumption 1: The dynamic characteristic of the high response proportional valve is assumed to be linear in this study. Therefore, the spool position is proportional to the applied signal, and the orifice open area s_0 of the pneumatic valve can be indicated by

$$s_0 = \pi_{sv}u \tag{7}$$

where π_{sv} is the coefficient factor and u is the control signal of the supply voltage.

Substituting (6) and (7) into (5), the dynamic equation of pneumatic spring can be illustrated as

$$\dot{P}_{as} = \frac{\kappa RT}{A_{as}\,(z_{as0}+x_1-x_3)}\left(\pi_{sv}q_{as}u-\frac{P_{as}A_{as}\,(x_2-x_4)}{RT}\right) \tag{8}$$

Consider $x_5 = (A_{as}/m_s)P_{as}$, we can obtain (8) by

$$\dot{x}_5 = \frac{\kappa RT}{m_s\,(z_{as0}+x_1-x_3)}\pi_{sv}q_{as}u - \frac{\kappa}{(z_{as0}+x_1-x_3)}x_5\,(x_2-x_4) \tag{9}$$

To enhance the tracking control, it is necessary to consider the full dynamic behavior of the pneumatic system, especially the nonlinear pneumatic stiffness k_p of the air bellow. Although some simulation methods can determine this parameter based on the thermodynamic theory [50], its application to the controller design is not easy because it depends on various working conditions and external disturbances. Thus, this stiffness coefficient is considered as an uncertain parameter in this study and we can specify the unknown function from (3) as

$$d_2\,(t) = \frac{1}{m_s}\left[-k_p(x_1-x_3)\right] \tag{10}$$

On the other hand, the air pressure of pneumatic spring is a high nonlinearity parameter which is affected by the unmodeled dynamics and the behavior of the twisted cord rubber material under the effect of external forces. Therefore, the dynamic model (9) should consider the unmodeled term of internal pressure when applying for the control design process.

Control Objectives: The active suspension system is designed to meet three objectives

1) Passenger comfort: The proposed control is applied to stabilize chassis displacement, thereby enhancing the comfort of the passenger.
2) Driving safety: This objective guarantees that the tires are always in contact with the road surface. To satisfy this condition, the relative tire fore (RTF) must be maintained to be less than 1.

$$RTF = \frac{F_t}{[m_s+m_{us}]\,g} \tag{11}$$

1) Handling stability: The suspension space must be smaller than the limitations of the mechanical architecture. For this purpose, the relative suspension deflection (RSD) is defined by

$$RSD = \frac{z_s-z_{us}}{z_R} \tag{12}$$

where z_R is the maximum value of the suspension displacement.

Remark 1: Some controllers are designed to satisfy the three above requirements, but these objectives conflict with each other because increasing the passenger comfort will require a larger oscillation. Thus, the proposed control in this study not only solves this problem by providing the PPF constraint but also considers the actuator failures of the pneumatic system.

B. FAULT PROBLEM MODEL AND PRELIMINARIES

It is well-known that actuator faults could limit the system performance of the pneumatic active suspension. To deal with this problem, the actuator failures are considered in this article, which can be modeled as [51]. Two types of lock-in-place and loss of effectiveness model are examined in the controller.

1) Lock-in-place model: This case shows the fact that the actuator gets stuck at a time t and it can be described by

$$u_i = \hbar \tag{13}$$

where $\hbar$ is a constant denotes the float fault of the actuator.

2) Loss of effectiveness model:

$$u_i = \lambda u_f \tag{14}$$

where u_f represents the actual input signal and $\lambda \in (0, 1]$ denotes the ratio of the actuator that remains effective after losing some effectiveness. For example, $\lambda = 0.6$ means that the actual coefficient actuator is 60% and the actuator losses 40%. When $\lambda = 1$, the actuator operates with the normal condition (no faults occur).

Basing on two cases of actuator failures, we can describe the general form of fault as follows

$$u = \lambda u_f + \hbar \tag{15}$$

Remark 2: Note with the lock-in-place model, it means that $\lambda = 0$ and $\hbar \neq 0$ while the loss of effectiveness model is represented by $\lambda \in (0, 1]$.

Generally, considering the dynamic model of pneumatic spring (9) with unmodeled parameters, external disturbance, unknown function (10), and actuator fault (15), we can write the full state space form of the pneumatic suspension model as

$$\begin{aligned}
\dot{x}_1 &= x_2 \\
\dot{x}_2 &= x_5 + \frac{1}{m_s}\left[-k_s(x_1-x_3)-c_d(x_2-x_4)\right]+d_2\,(t) \\
\dot{x}_3 &= x_4 \\
\dot{x}_4 &= \frac{1}{m_{us}}\begin{bmatrix} -k_{st}(x_3-z_r)-c_{dt}(x_4-\dot{z}_r) \\ +k_s(x_1-x_3)+c_d(x_2-x_4)-m_s x_5 \end{bmatrix} - \frac{m_s}{m_{us}}d_2\,(t) \\
\dot{x}_5 &= \frac{\kappa RT}{m_s\,(z_{as0}+x_1-x_3)}\pi_{sv}q_{as}\left(\lambda u_f+\hbar\right) \\
&\quad - \frac{\kappa}{(z_{as0}+x_1-x_3)}x_5\,(x_2-x_4)+p\,(t)
\end{aligned} \tag{16}$$

where $p\,(t)$ is the time-varying modeling error of air bellow pressure.

To guarantee comfort for the passenger, the controller will be designed to dissipate the external excitation into the chassis. For this purpose, we focus on the dynamic equations of

the sprung mass as follows

$$\begin{aligned}\dot{x}_1 &= x_2\\ \dot{x}_2 &= f_2+g_2x_5+d_2\,(t)\\ \dot{x}_5 &= f_3+g_3u_f+D_3\,(t)\end{aligned} \tag{17}$$

where $f_2 = 1/m_s[-k_s(x_1-x_3)-c_d(x_2-x_4)]$, $g_2 = 1, f_3 = [-\kappa/(z_{as0}+x_1-x_3)](x_2-x_4)x_5$, $D_3(t) = p(t)+g_3\hbar/\lambda$, $g_3 = \{\kappa RT/[m_s(z_{as0}+x_1-x_3)]\}\pi_{sv}q_{as}\lambda$.

Based on the dynamic equation (17), we can see that f_2 and f_3 are unknown smooth functions because x_3, x_4 are not considered in the control design. Besides, the damping characteristic of the pneumatic spring cannot be accurately simulated, and it is usually neglected in the suspension models. These problems will be solved by the control design based on the following preliminaries.

Assumption 2: Under the limitation of mechanical structure and physical performance, the sprung mass is assumed to be bounded by $m_{s\min} < m_s < m_{s\max}$, where $m_{s\max}$ and $m_{s\min}$ denote the upper and lower bound, respectively.

Remark 3: The sprung mass m_s is an unknown variable depending on the various masses of passengers. Thus, the unknown function g_3 contains the parametric uncertainties and it can be considered as time-varying control gains.

FLSs have been shown to be a good approximation technique for the unknown continuous functions. The FLSs are composed of a fuzzy rule base, a fuzzifier, a fuzzy inference engine, and a defuzzifier. The knowledge base constitutes a series of fuzzy If-Then rules as follows

$$\begin{aligned}&R^l:\ \text{If } x_1 \text{ is } H_1^l \text{ and } x_2 \text{ is } H_2^l \text{ and } \ldots\ x_n \text{ is } H_n^l,\ \text{then}\\ &y \text{ is } T^l,\ l = 1, \ldots, N\end{aligned} \tag{18}$$

where $X = [x_1, x_2, \ldots, x_n]^T$ and y are the FLSs input and output; H_i^l and T^l are fuzzy sets associated with fuzzy membership functions $\theta_{H_i^l}(x_i)$ and $\theta_{T^l}(y)$; and N is the number of fuzzy rules [52].

Through singleton fuzzifier, center average defuzzification, and product inference, the FLSs can be expressed as

$$y(X) = \frac{\sum_{l=1}^{N}\bar{y}_l\prod_{i=1}^{n}\theta_{H_i^l}(X_i)}{\sum_{l=1}^{N}\left(\prod_{i=1}^{n}\theta_{H_i^l}(X_i)\right)} \tag{19}$$

where $\bar{y}_l = \max_{y\in R}\left\{\theta_{T^l}(y)\right\}$.

Then, the fuzzy basic function can be designed by

$$s_l = \frac{\prod_{i=1}^{n}\theta_{H_i^l}(X_i)}{\sum_{l=1}^{N}\left(\prod_{i=1}^{n}\theta_{H_i^l}(X_i)\right)} \tag{20}$$

Determine $S(X) = [s_1(X), s_2(X), \ldots, s_N(X)]^T$ and $W^T = [\bar{y}_1, \bar{y}_2, \ldots, \bar{y}_N] = [w_1, w_2, \ldots, w_N]$, one can obtain the fuzzy logic (19) as follows

$$y(X) = W^TS(X) \tag{21}$$

Lemma 1 [53]: Define a continuous vector function $f(X)$ on a compact set Ω, for any given positive constant $\eta > 0$, there exist fuzzy logic systems $W^TS(X)$ that satisfy

$$\sup_{X\in\Omega}\left|f(X)-W^TS(X)\right| \le \eta \tag{22}$$

where $\eta > 0$ is an error value of the fuzzy system approximation to an unknown function, W is the ideal FLSs weight matrix, and $S(X)$ is bounded by $\|S(X)\| \le \iota$.

In the following, the FLSs are used to approximate the unknown functions $f(X)$ with $X \in \Omega$

$$f_i(X) = W_i^TS_i(X_i)+\eta_i \tag{23}$$

Lemma 2 [32]: The command filter is employed to eliminate the derivative of the virtual control of traditional backstepping as follows

$$\begin{aligned}\dot{\theta}_{i1} &= \rho_m\theta_{i2}\\ \dot{\theta}_{i2} &= -2\tau_m\rho_m\theta_{i2}-\rho_m(\theta_{i1}-\alpha_{i-1})\end{aligned} \tag{24}$$

where ρ_m and τ_m are the control parameters and α_{i-1} are the virtual control signals. The output of each filter is chosen by $x_i^c = \theta_{i1}$ and $\dot{x}_i^c = \dot{\theta}_{i1}$. Let the input signal α_{i-1} and their derivatives are bounded and satisfied $|\dot{\alpha}_{i-1}| \le \ell_1$ and $|\ddot{\alpha}_{i-1}| \le \ell_2$ in a finite time, there exist $\tau_m \in (0, 1]$ and $\rho_m > 0$ so that the following inequality holds

$$\left|x_i^c-\alpha_{i-1}\right| \le \ell_3 \tag{25}$$

where $\ell_i > 0, i = 1, 2, 3$ are the positive constants.

Remark 4: The command filter control (24) is designed to compute the intermediate control signal x_{ic} and $\dot{x}_{ic}$ without a differentiator. Hence, the explosion of complexity problem in the basic backstepping technique is solved.

Lemma 3 [32]: To decline the effect of the command filter errors $(\theta_{i1}-\alpha_{i-1})$, the compensation mechanisms φ_i are employed at each step of the control design process.

$$\begin{aligned}\dot{\varphi}_1 &= -k_1\varphi_1+g_1\varphi_2+g_1\left(x_2^c-\alpha_1\right)\\ \dot{\varphi}_i &= -k_i\varphi_i-g_{i-1}\varphi_{i-1}+g_i\varphi_{i+1}+g_i\left(x_{i+1}^c-\alpha_i\right)\\ \dot{\varphi}_n &= -k_n\varphi_n-g_{n-1}\varphi_{n-1}\end{aligned} \tag{26}$$

where the initial condition is selected $\varphi_i(0) = 0$ for $t \in [0, T_1]$, and k_i are design parameters.

The compensation mechanisms are bounded by invoking [54]

$$\|\varphi_i(t)\| \le \frac{\ell_3\bar{G}_{31}}{2k_0}\left(1-e^{-2k_0(t-T_1)}\right) \tag{27}$$

where $k_0 = (1/2)\,min\,(k_i)$

III. ADAPTIVE FUZZY OBSERVER-BASED FAULT TOLERANT CONTROLLER

A. ADAPTIVE FUZZY OBSERVER COMMAND FILTERED CONTROL WITH PRESCRIBED PERFORMANCE

This section proposes an adaptive fuzzy observer fault tolerant control scheme based on the command filtered backstepping technique. The FLSs are employed to approximate the unknown functions while the nonlinear disturbance observer

is used to handle the effects of the actuator failures, approximation errors, and external disturbances. The PPF constraint is used to ensure the tracking error of vertical displacement does not violate the boundary. Finally, the Lyapunov theorem is applied to analyze the stability of the proposed control scheme.

Step 1: In this step, the tracking error constraint of vertical displacement is guaranteed by the PPF. First, we define the tracking error of sprung mass displacement by

$$e_1 = x_1 - x_d \tag{28}$$

where x_d is the reference trajectory.

Definition 2 [20]: The prescribed performance is defined by a positive smooth function $\delta(t)$

$$\delta(t) = (\delta_0 - \delta_\infty) e^{-\phi t} + \delta_\infty \tag{29}$$

where δ_0 indicates the initial value, δ_∞ denotes the ultimate error, and $\phi > 0$ is the convergence rate. The initial conditions are chosen to satisfy $\lim_{t\to 0} \delta(t) = \delta_0 > 0$, $\lim_{t\to\infty} \delta(t) = \delta_\infty > 0$, and $\rho_0 > \rho_\infty$.

The PPF (29) is used to establish the predefined boundaries which retain the tracking error e_1 by the following inequality

$$-\vartheta\delta(t) < e_1 < \bar{\vartheta}\delta(t) \tag{30}$$

where $\vartheta, \bar{\vartheta} > 0$ are the positive design parameters.

Remark 5: It can be seen from (29) and (30), the lower bound of tracking error is determined by $-\vartheta\delta(0)$ while $\bar{\vartheta}\delta(0)$ stands for the upper bound. Thus, the steady-state performance of tracking error can be satisfied by choosing the appropriate control parameters $\delta_0, \delta_\infty, \phi, \vartheta, \bar{\vartheta}$.

To combine the PPF into the proposed control, the constrained transformation technique is applied to convert the prescribed performance boundary into an equality form. Hence, one can use a smooth and strictly increasing function $G(z_1)$ which is given by [20].

$$G(z_1) = \frac{\bar{\vartheta} e^{z_1} - \vartheta e^{-z_1}}{e^{z_1} + e^{-z_1}} \tag{31}$$

Furthermore, the function $G(z_1)$ satisfies: $-\vartheta < G(z_1) < \bar{\vartheta}$ and $\lim_{z_1\to\infty} G(z_1) = \bar{\vartheta}$, $\lim_{z_1\to-\infty} G(z_1) = -\vartheta$. Then, the inequality condition (30) can be converted by the following form

$$e_1 = \delta(t) G(z_1) \tag{32}$$

Then, one can obtain the inverse transfer function z_1 as follows

$$z_1 = G^{-1}\left(\frac{e_1}{\delta(t)}\right) \tag{33}$$

Set $\chi = e_1/\delta(t)$, the transform function z_1 can be written by

$$z_1 = \frac{1}{2}\ln\left(\frac{\chi+\vartheta}{\bar{\vartheta}-\chi}\right) \tag{34}$$

Lemma 4 [55]: According to the above analysis, the transform function z_1 of the system state is transferred by the smooth function $G(z_1)$ and the stability of the tracking error e_1 can be ensured within the predefined boundaries (30).

Remark 6: The control parameters $\vartheta, \bar{\vartheta}, \delta_0, \delta_\infty, \phi$ are chosen for the PPF constraint (29) and error transform $G(z_1)$ when we design the controller. As the parameters $\vartheta, \bar{\vartheta}, \delta_0$ are selected to satisfy the initial condition $-\vartheta\delta(0) < x_1(0) < \bar{\vartheta}\delta(0)$, the transfer function z_1 can be restrained within the boundaries. Hence, the condition $-\vartheta < G(z_1) < \bar{\vartheta}$ is held and the tracking error $-\vartheta\delta(t) < e_1 < \bar{\vartheta}\delta(t)$ is guaranteed.

Step 2: Choose the virtual control α_1

We obtain the time derivative of z_1 from (34) as follows

$$\dot{z}_1 = \frac{1}{2}\left(\frac{1}{\chi+\vartheta} - \frac{1}{\chi-\bar{\vartheta}}\right)\left(\frac{\dot{x}_1}{\delta} - \frac{x_1\dot{\delta}}{\delta^2}\right) = \zeta\left(x_2 - \frac{x_1\dot{\delta}}{\delta}\right) \tag{35}$$

where $\zeta = \frac{1}{2\delta}\left(\frac{1}{\chi+\vartheta} - \frac{1}{\chi-\bar{\vartheta}}\right)$

Choose a candidate Lyapunov function $V_1 = (1/2) z_1^2$. Thus, the time derivative of V_1 is calculated

$$\dot{V}_1 = z_1\dot{z}_1 \tag{36}$$

Based on the traditional backstepping technique in this step, we obtain $\dot{V}_1$ as follows

$$\dot{V}_1 = \zeta z_1\left(z_2 + \alpha_1 - \frac{x_1\dot{\delta}}{\delta}\right) \tag{37}$$

Select the virtual control α_1 by

$$\alpha_1 = -\zeta^{-1}k_1 z_1 + \frac{x_1\dot{\delta}}{\delta} \tag{38}$$

Using (38), we can write (37) as follows

$$\dot{V}_1 = -k_1 z_1^2 + \zeta z_1 z_2 \tag{39}$$

Step 3: Choose the virtual control α_2

In this step, the command filtered backstepping algorithm is employed to design the control scheme, and the tracking error of x_2 is defined by

$$e_2 = x_2 - x_2^c \tag{40}$$

where x_2^c denotes the output signal of the command filter through the virtual controller α_1.

We can define the compensated tracking error

$$z_2 = e_2 - \varphi_2 \tag{41}$$

The error compensation is designed by (26)

$$\dot{\varphi}_2 = -k_2\varphi_2 + g_2\varphi_3 + g_2\left(x_3^c - \alpha_2\right) \tag{42}$$

where x_3^c is the output signal of the command filter through the virtual controller α_2, which is determined later.

Therefore, we can express the time derivative of z_2 by using (17)

$$\dot{z}_2 = f_2 + g_2 x_5 + d_2(t) - \dot{x}_2^c - \dot{\varphi}_2 \tag{43}$$

Based on Lemma 1, the unknown function f_2 is approximated by FLSs, we have: $f_2 = W_2^T S_2(X_2) + \eta_2(X_2)$, where $X_2 = [x_1, x_2]^T$. Then, we can write (43) as follows

$$\dot{z}_2 = W_2^T S_2(X_2) + \eta_2(X_2) + g_2 x_5 + d_2(t) - \dot{x}_2^c - \dot{\varphi}_2 \tag{44}$$

Define the approximate error $\eta_2(X_2)$ and uncertain parameter $d_2(t)$ by using the unknown function $D_2(t) = \eta_2(X_2)+d_2(t)$, we can arrange (44) again

$$\dot{z}_2 = W_2^T S_2(X_2)+g_2x_5+D_2(t)-\dot{x}_2^c-\dot{\varphi}_2 \tag{45}$$

Substituting (42) into (45), we can obtain

$$\dot{z}_2 = W_2^T S_2(X_2)+g_2x_5+D_2(t)-\dot{x}_2^c+k_2\varphi_2-g_2\varphi_3 -g_2\left(x_3^c-\alpha_2\right) \tag{46}$$

Choose the virtual control α_2

$$\alpha_2 = \frac{1}{g_2}\left(-\zeta z_1-\hat{W}_2^T S_2(X_2)-\hat{D}_2+\dot{x}_2^c-k_2e_2\right) \tag{47}$$

where $\hat{D}_2$ is the estimation of the disturbance $D_2(t)$ and $\hat{W}_2$ is the estimation of the ideal weight vector W_2.

Besides, the adaptive law is proposed as

$$\dot{\hat{W}}_2 = \beta_2\left(z_2S_2(X_2)-\varsigma_2\hat{W}_2\right) \tag{48}$$

where $\beta_2 > 0$ and $\varsigma_2 > 0$ are the design parameters.

Substitute (47) into (46), we have

$$\dot{z}_2 = -\zeta z_1+\tilde{W}_2^T S_2(X_2)+\tilde{D}_2-k_2z_2+g_2z_3 \tag{49}$$

where $\tilde{D}_2 = D_2-\hat{D}_2$ is the error of disturbance observer and $\tilde{W}_2 = W_2-\hat{W}_2$ is the error of weight estimation.

From (49), we obtain

$$z_2(\zeta z_1+\dot{z}_2) = z_2\left(\tilde{W}_2^T S_2(X_2)+\tilde{D}_2-k_2z_2+g_2z_3\right) \tag{50}$$

To estimate the disturbance $D_2(t)$, the fuzzy nonlinear disturbance observer is designed by

$$\begin{aligned}\hat{D}_2 &= z_2-\lambda_2\\ \dot{\lambda}_2 &= g_2x_5+\hat{W}_2^T S_2(X_2)+\hat{D}_2-\dot{x}_2^c-\dot{\varphi}_2\end{aligned} \tag{51}$$

Using (45) and (51), we obtain

$$\dot{\hat{D}}_2 = \tilde{W}_2^T S_2(X_2)+\tilde{D}_2 \tag{52}$$

Then, the time derivate of disturbance error can be derived as follows

$$\dot{\tilde{D}}_2 = \dot{D}_2-\dot{\hat{D}}_2 = \dot{D}_2-\tilde{D}_2-\tilde{W}_2^T S_2(X_2) \tag{53}$$

The candidate Lyapunov function V_2 is selected by

$$V_2 = V_1+\frac{1}{2}z_2^2+\frac{1}{2}\beta_2^{-1}\tilde{W}_2^T\tilde{W}_2+\frac{1}{2}\tilde{D}_2^2 \tag{54}$$

Taking the time derivative of V_2 using (39), we have

$$\dot{V}_2 = -k_1z_1^2+z_2(\zeta z_1+\dot{z}_2)+\beta_2^{-1}\tilde{W}_2^T\dot{\tilde{W}}_2+D_2\dot{\tilde{D}}_2 \tag{55}$$

Using (50) and (53), we can write (55) as

$$\dot{V}_2 = -k_1z_1^2-k_2z_2^2+z_2\tilde{W}_2^T S_2(X_2)+z_2\tilde{D}_2+g_2z_2z_3 -\beta_2^{-1}\tilde{W}_2^T\dot{\hat{W}}_2+\tilde{D}_2\left(\dot{D}_2-\tilde{D}_2-\tilde{W}_2^T S_2(X_2)\right) \tag{56}$$

Substituting (48) into (56), we have

$$\dot{V}_2 = -k_1z_1^2-k_2z_2^2+z_2\tilde{D}_2+g_2z_2z_3+\varsigma_2\tilde{W}_2^T\hat{W}_2 +\tilde{D}_2\dot{D}_2-\tilde{D}_2^2-\tilde{D}_2\tilde{W}_2^T S_2(X_2) \tag{57}$$

Step 4: Design the fault tolerant control signal u_f

Similar to step 3, the tracking error of x_5 can be defined by

$$e_3 = x_5-x_3^c \tag{58}$$

Then we can calculate the compensated tracking error

$$z_3 = e_3-\varphi_3 \tag{59}$$

From (26), the compensating signals is used

$$\dot{\varphi}_3 = -k_3\varphi_3-g_2\varphi_2 \tag{60}$$

Using (17) and (58), we can obtain the time derivative of z_3 as follows

$$\dot{z}_3 = f_3+g_3u_f+D_3(t)-\dot{x}_3^c-\dot{\varphi}_3 \tag{61}$$

Therefore, we can choose the desired control u_f^d

$$u_f^d = -k_3z_3-D_3(t)-z_2-\frac{1}{g_3}\left(f_3-\dot{x}_3^c-\dot{\varphi}_3\right) \tag{62}$$

Approximate the unknown function $(f_3-\dot{x}_3^c-\dot{\varphi}_3)/g_3$ by FLSs, we have: $(f_3-\dot{x}_3^c-\dot{\varphi}_3)/g_3 = W_3^T S_3(X_3)+\eta_3(X_3)$, where $X_2 = [x_1, x_2, x_5]^T$. Hence, we can write (62) as follows

$$u_f^d = -k_3z_3-D_3(t)-z_2-W_3^T S_3(X_3)-\eta_3(X_3) \tag{63}$$

Then, the adaptive fault tolerant control with disturbance observer is proposed by

$$u_f = -k_3z_3-\hat{D}_3-z_2-\hat{W}_3^T S_3(X_3) \tag{64}$$

where $\hat{D}_3$ the estimation of the disturbance $D_3(t)$.

The adaptive law is designed as

$$\dot{\hat{W}}_3 = \beta_3\left(z_3S_3(X_3)-\varsigma_3\hat{W}_3\right) \tag{65}$$

where $\beta_3 > 0$ and $\varsigma_3 > 0$ are the design parameters.

Substituting (64) into (61), we obtain

$$\dot{z}_3 = g_3\left(-k_3z_3+\tilde{W}_3^T S_3(X_3)-\hat{D}_3-z_2+\eta_3(X_3)\right)+D_3(t) \tag{66}$$

In this step, the fuzzy nonlinear disturbance observer is designed for FTC as follows

$$\hat{D}_3 = \upsilon_3(\mu_3-\varpi_3) \tag{67}$$

where υ_3 is control parameter, μ_3 and ϖ_3 are the auxiliary variable and the intermedial variable, which are defined by

$$\mu_3 = z_3-\lambda_3 \tag{68}$$

$$\dot{\varpi}_3 = \hat{D}_3-b_3\mu_3 \tag{69}$$

where $b_3 > 0$ is the design parameter.

The intermedial variable λ_3 is proposed by

$$\dot{\lambda}_3 = b_3\mu_3+\upsilon_3^{-1}\hat{W}_F^T S_F(X_F)-\dot{x}_3^c-\dot{\varphi}_3 \tag{70}$$

And define the adaptive law $\hat{W}_F$

$$\dot{\hat{W}}_F = \beta_F\left(\upsilon_3^{-1}\mu_3S_F(X_F)-\varsigma_F\hat{W}_F\right) \tag{71}$$

where $\beta_F > 0$ and $\varsigma_F > 0$ are control parameters.

To design the disturbance observer for FTC, we set $F_F(X_F) = \upsilon_3(f_3+g_3u_f)$ from the equation (61), where $X_F = [x_1, x_2, x_5, u_f]^T$

$$\dot{z}_3 = \upsilon_3^{-1}F_F(X_F)+D_3(t)-\dot{x}_3^c-\dot{\varphi}_3 \tag{72}$$

where $\upsilon_3 > 0$ is the design parameter.

By employing FLSs for $F_F(X_F) = W_F^T S_F(X_F)+\varepsilon_F(X_F)$, we obtain

$$\dot{z}_3 = \upsilon_3^{-1}W_F^T S_F(X_F)+\upsilon_3^{-1}\varepsilon_F(X_F)+D_3(t)-\dot{x}_3^c-\dot{\varphi}_3 \tag{73}$$

Differentiating (68) using (70) and (73), we have

$$\dot{\mu}_3 = \upsilon_3^{-1}\tilde{W}_F^T S_F(X_F)+\upsilon_3^{-1}\eta_F(X_F)+D_3(t)-b_3\mu_3 \tag{74}$$

where $\tilde{W}_F = \hat{W}_F-W_F$. Then, we obtain

$$\mu_3\dot{\mu}_3 = \mu_3\upsilon_3^{-1}\tilde{W}_F^T S_F(X_F)+\mu_3\upsilon_3^{-1}\eta_F(X_F) +\mu_3 D_3(t)-b_3\mu_3^2 \tag{75}$$

Basing on Young's inequality theorem for nonnegative real numbers a and b, we have $ab \le a^2/(2\rho)+(b^2\rho)/2$, where $\rho > 0$ is the adjustable parameter. Hence, we can obtain

$$\mu_3\dot{\mu}_3 \le \mu_3\upsilon_3^{-1}\tilde{W}_F^T S_F(X_F)+\frac{1}{2}\upsilon_3^{-2}\eta_F^2(X_F) +\frac{1}{2}D_3^2-(b_3-1)\mu_3^2 \tag{76}$$

Similarity, we can obtain the time derivative of $\hat{D}_3$ from (67), (69), and (74) as follows

$$\dot{\hat{D}}_3 = \tilde{W}_F^T S_F(X_F)+\eta_F(X_F)+\upsilon_3\tilde{D}_3 \tag{77}$$

Therefore, we can obtain the disturbance error

$$\dot{\tilde{D}}_3 = \dot{D}_3-\dot{\hat{D}}_3 = \dot{D}_3-\tilde{W}_F^T S_F(X_F)-\eta_F(X_F)-\upsilon_3\tilde{D}_3 \tag{78}$$

And

$$\tilde{D}_3\dot{\tilde{D}}_3 = \tilde{D}_3\dot{D}_3-\tilde{D}_3\tilde{W}_F^T S_F(X_F)-\tilde{D}_3\eta_F(X_F)-\upsilon_3\tilde{D}_3^2 \tag{79}$$

Theorem: The virtual controllers (38), (47), fuzzy disturbance observers (51), (67), adaptive fault tolerant control (64), and adaptation laws (48), (65), and (71) are designed for the system (17) under Assumptions 1, 2. The developed fault tolerant control scheme can ensure that all state variables of the active suspension are semi-global uniformly ultimately bounded and the tracking errors converge to a sufficiently small neighborhood of the origin. Moreover, the goal of actuator failures is achieved while the transient performance of vertical displacement can be constrained within the specified PPF.

Proof: Choose the candidate Lyapunov function V_3 and V

$$V_3 = V_2+\frac{1}{2}z_3^2+\frac{1}{2}\beta_3^{-1}\tilde{W}_3^T\tilde{W}_3+\frac{1}{2}\tilde{D}_3^2 \tag{80}$$

$$V = V_3+\frac{1}{2}\beta_F^{-1}\tilde{W}_F^T\tilde{W}_F+\frac{1}{2}\mu_3^2 \tag{81}$$

We can derive the time derivative of V from (81) as follows

$$\dot{V} = \dot{V}_2+z_3\dot{z}_3-\beta_3^{-1}\tilde{W}_3^T\dot{\hat{W}}_3-\beta_F^{-1}\tilde{W}_F^T\dot{\hat{W}}_F+\tilde{D}_3\dot{\tilde{D}}_3+\mu_3\dot{\mu}_3 \tag{82}$$

Applying (57), (66), (76), and (79) into (82), one obtains the derivative of V as follows

$$\begin{aligned}\dot{V} \le\ & -k_1z_1^2-k_2z_2^2+z_2\tilde{D}_2+g_2z_2z_3+\varsigma_2\tilde{W}_2^T\hat{W}_2 \\ & +\tilde{D}_2\dot{D}_2-\tilde{D}_2^2-\tilde{D}_2\tilde{W}_2^T S_2(X_2)-\beta_3^{-1}\tilde{W}_3^T\dot{\hat{W}}_3 \\ & +z_3\left(-k_3z_3+\tilde{W}_3^T S_3(X_3)-\hat{D}_3-z_2+\eta_3(X_3)+D_3\right) \\ & +\left(\tilde{D}_3\dot{D}_3-\tilde{D}_3\tilde{W}_F^T S_F(X_F)-\tilde{D}_3\eta_F(X_F)-\upsilon_3\tilde{D}_3^2\right) \\ & -\beta_F^{-1}\tilde{W}_F^T\dot{\hat{W}}_F \\ & +\left(\mu_3\upsilon_3^{-1}\tilde{W}_F^T S_F(X_F)+\frac{1}{2}\upsilon_3^{-2}\eta_F^2(X_F)+\frac{1}{2}D_3^2-(b_3-1)\mu_3^2\right)\end{aligned} \tag{83}$$

Applying Young's inequality and (65), (71), we have

$$z_2\tilde{D}_2 \le \frac{1}{2}z_2^2+\frac{1}{2}\tilde{D}_2^2;\ \varsigma_2\tilde{W}_2^T\hat{W}_2 \le \frac{\varsigma_2}{2}\|W_2\|^2-\frac{\varsigma_2}{2}\left\|\tilde{W}_2\right\|^2$$

$$\tilde{D}_2\dot{D}_2 \le \frac{1}{2}\tilde{D}_2^2+\frac{1}{2}\dot{D}_2^2;\ \tilde{D}_2\tilde{W}_2^T S_2(X_2) \le \rho_2\tilde{D}_2^2\iota_2^2+\frac{1}{\rho_2}\left\|\tilde{W}_2\right\|^2$$

$$\begin{aligned}z_3\hat{D}_3 &= z_3D_3-z_3\tilde{D}_3; \\ z_3\eta_3(X_3) &\le \frac{1}{2}z_3^2+\frac{1}{2}\eta_3^2(X_3); \\ \tilde{D}_3\eta_F(X_F) &\le \frac{1}{2}\tilde{D}_3^2+\frac{1}{2}\eta_F^2(X_F); \\ \tilde{D}_3\dot{D}_3 &\le \frac{1}{2}\tilde{D}_3^2+\frac{1}{2}\dot{D}_3^2; \\ \tilde{D}_3\tilde{W}_F^T S_F(X_F) &\le \rho_F\tilde{D}_3^2\iota_F^2+\frac{1}{\rho_F}\left\|\tilde{W}_F\right\|^2\end{aligned}$$

Using (65) and (71), we receive

$$\begin{aligned}\beta_3^{-1}\tilde{W}_3^T\dot{\hat{W}}_3 &= z_3\tilde{W}_3^T S_3(X_3)-\varsigma_3\tilde{W}_3^T\hat{W}_3 \\ \beta_F^{-1}\tilde{W}_F^T\dot{\hat{W}}_F &= \upsilon_3^{-1}\mu_3\tilde{W}_F^T S_F(X_F)-\varsigma_3\tilde{W}_F^T\hat{W}_F\end{aligned}$$

So, we can write (83) as follows

$$\begin{aligned}\dot{V} =\ & -k_1z_1^2-k_2z_2^2-k_3z_3^2+\frac{1}{2}z_2^2+\frac{1}{2}\tilde{D}_2^2+\frac{\varsigma_2}{2}\|W_2\|^2-\frac{\varsigma_2}{2}\left\|\tilde{W}_2\right\|^2 \\ & +\frac{1}{2}\tilde{D}_2^2+\frac{1}{2}\dot{D}_2^2-\tilde{D}_2^2-\rho_2\tilde{D}_2^2\iota_2^2-\frac{1}{\rho_2}\left\|\tilde{W}_2\right\|^2+z_3\tilde{W}_3^T S_3(X_3) \\ & -z_3D_3+z_3\tilde{D}_3+\frac{1}{2}z_3^2+\frac{1}{2}\eta_3^2(X_3)+z_3D_3-(b_3-1)\mu_3^2 \\ & -z_3\tilde{W}_3^T S_3(X_3)+\varsigma_3\tilde{W}_3^T\hat{W}_3-\upsilon_3^{-1}\mu_3\tilde{W}_F^T S_F(X_F)+\varsigma_3\tilde{W}_F^T\hat{W}_F \\ & +\frac{1}{2}\tilde{D}_3^2+\frac{1}{2}\dot{D}_3^2-\rho_F\tilde{D}_3^2\iota_F^2-\frac{1}{\rho_F}\left\|\tilde{W}_F\right\|^2-\frac{1}{2}\tilde{D}_3^2-\frac{1}{2}\eta_F^2(X_F) \\ & -\upsilon_3\tilde{D}_3^2+\upsilon_3^{-1}\tilde{W}_F^T S_F(X_F)+\frac{1}{2}\upsilon_3^{-2}\eta_F^2(X_F)+\frac{1}{2}D_3^2\end{aligned}$$

We also apply Young's inequality to prove the following inequalities

$$\begin{aligned}\varsigma_3\tilde{W}_3^T\hat{W}_3 &\le \frac{\varsigma_3}{2}\|W_3\|^2-\frac{\varsigma_3}{2}\left\|\tilde{W}_3\right\|^2 \\ \beta_F^{-1}\tilde{W}_F^T\dot{\hat{W}}_F &= \upsilon_3^{-1}\mu_3\tilde{W}_F^T S_F(X_F)-\varsigma_3\tilde{W}_F^T\hat{W}_F\end{aligned} \tag{84}$$

Thus, we can arrange (84) as follows

$$\begin{aligned}\dot{V} = &-k_1 z_1^2-\left(k_2-\frac{1}{2}\right) z_2^2-\left(k_3-\frac{3}{2}\right) z_3^2+\frac{\varsigma_F}{2}\left\|W_F\right\|^2 \\ &-\left(b_3-1\right)\mu_3^2-\left(\frac{1}{\rho_2}+\frac{\varsigma_2}{2}\right)\left\|\tilde{W}_2\right\|^2-\frac{\varsigma_3}{2}\left\|\tilde{W}_3\right\|^2 \\ &-\left(\frac{1}{\rho_F}+\frac{\varsigma_F}{2}\right)\left\|\tilde{W}_F\right\|^2-\rho_2\iota_2^2\tilde{D}_2^2-\left(\rho_F\iota_F^2+\upsilon_3-\frac{1}{2}\right)\tilde{D}_3^2 \\ &+\frac{\varsigma_2}{2}\left\|W_2\right\|^2+\frac{\varsigma_3}{2}\left\|W_3\right\|^2+\frac{1}{2}\dot{D}_2^2+\frac{1}{2}D_3^2 \\ &+\frac{1}{2}\dot{D}_3^2+\frac{1}{2}\eta_3^2\left(X_3\right)-\left(\frac{1}{2}-\frac{1}{2}\upsilon_3^{-2}\right)\eta_F^2\left(X_F\right) \end{aligned} \tag{85}$$

By choosing the corresponding control parameters to satisfy the system conditions, we can determine the following elements as follows

$$\Pi = min\left\{\begin{array}{l} 2k_1, 2\left(k_2-\frac{3}{2}\right), 2\left(k_3-\frac{3}{2}\right), 2\left(b_3-1\right), \varsigma_3 \\ 2\left(\frac{1}{\rho_2}+\frac{\varsigma_2}{2}\right), 2\left(\frac{1}{\rho_F}+\frac{\varsigma_F}{2}\right), \rho_2\iota_2^2, \\ \left(\rho_F\iota_F^2+\upsilon_3-\frac{1}{2}\right) \end{array}\right\} \tag{86}$$

$$\begin{aligned}\Psi = &\frac{\varsigma_2}{2}\left\|W_2\right\|^2+\frac{\varsigma_3}{2}\left\|W_3\right\|^2+\frac{\varsigma_F}{2}\left\|W_F\right\|^2+\frac{1}{2}\dot{D}_2^2+\frac{1}{2}\dot{D}_3^2 \\ &+\frac{1}{2}D_3^2+\frac{1}{2}\eta_3^2\left(X_3\right)-\left(\frac{1}{2}-\frac{1}{2}\upsilon_3^{-2}\right)\eta_F^2\left(X_F\right)\end{aligned} \tag{87}$$

And we can simplify (85) as follows

$$\dot{V} \le -\Pi V+\Psi \tag{88}$$

Multiplying (88) by $e^{\Pi t}$ on both sides and then integrating, we receive

$$\begin{aligned} &e^{\Pi t}\dot{V}+\Pi e^{\Pi t}V \le e^{\Pi t}\Psi \\ &\int_0^t\left(e^{\Pi t}V\right)^{\cdot}dt \le \Psi\int_0^t e^{\Pi t}dt \end{aligned} \tag{89}$$

$$V\left(t\right) \le \left(V\left(0\right)-\frac{\Psi}{\Pi}\right)e^{-\Pi t}+\frac{\Psi}{\Pi} \le V\left(0\right)e^{-\Pi t}+\frac{\Psi}{\Pi} \tag{90}$$

Therefore, we can conclude the following conditions according to (81),

$$\left|z_i\right| \le \sqrt{2\left(V\left(0\right)e^{-\Pi t}+\frac{\Psi}{\Pi}\right)}, \quad i=1,2,3 \tag{91}$$

It can be seen that transformation errors $z_i, i = 1, 2, 3$ and compensate signals $\varphi_i, i = 1, 2, 3$ are bounded, hereby the tracking errors e_1, e_2, e_3 are also bounded. Therefore, by selecting the control parameters and PPF constraints, the stability of the closed-loop system is guaranteed.

Remark 7: The external disturbances, unmodeled dynamics, and unknown coefficient of actuator failures are compensated by fuzzy logic systems and nonlinear disturbance observers. Here, the propped control is designed by the combination of the command filter technique and prescribed performance constraint theory. It not only reduces the computational complexity but also enhances the suspension performance in the presence of unknown parameters and actuator fault.

B. HANDLING STABILITY AND DRIVING SAFETY ANALYSIS

Based on the above results, the first objective of passenger comfort has been satisfied by the proposed control. Besides, two objectives of handling stability and driving safety can be ensured by choosing suitable design parameters that will be analyzed in this section. For these purposes, we concentrate on analyzing the dynamic equations of unsprung mass (16). Besides, the tracking errors $e_i, i = 1, 2, 3$ are assumed to be bounded according to (91). Applying the FLSs for $f_2 = W_2^T S_2\left(X_2\right)+\eta_2\left(X_2\right)$, we obtain (16) as follows

$$\dot{X} = CX+DY+Y_0 \tag{92}$$

where

$$X = \begin{bmatrix} x_3 \\ x_4 \end{bmatrix}; \quad C = \begin{bmatrix} 0 & 1 \\ -\frac{k_{st}}{m_{us}} & -\frac{c_{dt}}{m_{us}} \end{bmatrix};$$

$$D = \begin{bmatrix} 0 & 0 \\ \frac{k_{st}}{m_{us}} & \frac{c_{dt}}{m_{us}} \end{bmatrix}; \quad Y = \begin{bmatrix} z_r \\ \dot{z}_r \end{bmatrix}; \; Y_0 = \begin{bmatrix} 0 \\ M \end{bmatrix};$$

$$\mathrm{M} = \frac{m_s}{m_{us}}\left(W_2^T S_2\left(X_2\right)+\eta_2\left(X_2\right)\right)+\frac{1}{m_{us}}\left(-m_s x_5-m_s d_2\left(t\right)\right)$$

According to (91), we can see that M is bounded because the tracking errors z_1, z_2, and z_3 are bounded. There exists a constant $\bar{M}$ so that $\|M\| \le \bar{M}$ is hold.

The candidate Lyapunov function is chosen by

$$V_D = X^T PX \tag{93}$$

where P is a positive definite symmetric matrix.

Thus, we can obtain the time derivative of V_D

$$\dot{V}_D = \dot{X}^T PX+X^T P\dot{X} \tag{94}$$

Rewrite (94) using (92), we have

$$\dot{V}_D = X^T\left(C^T P+PC\right)X+2X^T PDY+2X^T PY_0 \tag{95}$$

There exists a positive definite symmetric matrix $Q > 0$ that satisfies the equation $C^T P+PC = -Q$. Besides, we can write the form of $2X^T PDY$ and $2X^T PY_0$ according to Young's inequality theorem as follows

$$\begin{aligned} 2X^T PDY &\le \frac{1}{\rho_1}X^T PDD^T PX+\rho_1 Y^T Y \\ 2X^T PY_0 &\le \frac{1}{\rho_2}X^T PPX+\rho_2 Y_0^T Y_{.0} \end{aligned} \tag{96}$$

where $\rho_i > 0, i = 1, 2$ are adjustable parameters.

Substituting (96) into (95), we have

$$\begin{aligned} &\dot{V}_D \\ &\le -\left[\begin{array}{l} \lambda_{\min}\left(P^{-1/2}QP^{-1/2}\right)-\frac{1}{\rho_1}\lambda_{\max}\left(P^{1/2}DD^T P^{1/2}\right) \\ -\frac{1}{\rho_2}\lambda_{\max}\left(P\right) \end{array}\right]V_D \\ &\quad +\rho_1 Y^T Y+\rho_2 Y_0^T Y_0 \end{aligned} \tag{97}$$

where $\lambda_{\max}$ and $\lambda_{\min}$ are the maximal and minimal eigenvalues of the matrix.

We can select the appropriate matrix P, Q to meet the following inequalities

$$\rho_1 > 2\frac{\lambda_{\max}\left(P^{1/2}DD^TP^{1/2}\right)}{\lambda_{\min}\left(P^{-1/2}QP^{-1/2}\right)}; \rho_2 > 2\frac{\lambda_{\max}(P)}{\lambda_{\min}\left(P^{-1/2}QP^{-1/2}\right)} \tag{98}$$

Based on (98), we can determine two parameters Υ and Δ such that

$$\Theta \geq \lambda_{\min}\left(P^{-1/2}QP^{-1/2}\right) - \frac{1}{\rho_1}\lambda_{\max}\left(P^{1/2}DD^TP^{1/2}\right) - \frac{1}{\rho_2}\lambda_{\max}(P) \tag{99}$$

$$\Phi \geq \rho_1 Y^T Y + \rho_2 Y_0^T Y_0 \tag{100}$$

Hence, we can rewrite the inequality (97) as follows

$$\dot{V}_D \leq -\Theta V_D + \Phi \tag{101}$$

Multiplying (101) by $e^{\Theta t}$ on both sides and integrating, we can write

$$V_D \leq \left(V_D(0) - \frac{\Phi}{\Theta}\right)e^{-\Theta t} + \frac{\Phi}{\Theta} \leq V_D(0)\,e^{-\Theta t} + \frac{\Phi}{\Theta} \tag{102}$$

According to (93), the system states (16) are bounded by

$$|x_i(t)| \leq \sqrt{\left(V_D(0)\,e^{-\Theta t} + \frac{\Phi}{\Theta}\right)/\lambda_{\min}(P)}, \quad i = 3, 4 \tag{103}$$

Substituting (103) into the handing stability (12), we can get

$$|z_s - z_{us}| \leq |x_1| + |x_3| \leq \bar{\vartheta}\,\delta(0) + \sqrt{\left(V_D(0)\,e^{-\Theta t} + \frac{\Phi}{\Theta}\right)/\lambda_{\min}(P)} \tag{104}$$

From (104), the handling stability condition can be guaranteed by choosing control parameters ρ_1, ρ_2, P, and the approximate PPF constraint $\bar{\vartheta}, \vartheta, \delta_0$ so that $|z_s - z_{us}| \leq z_R$.

Besides, the tire forces F_{st} and F_{dt} can be expressed by

$$\begin{aligned} F_{st}(z_{us}, z_r, t) &= k_{st}(x_3 - z_r) \\ &\leq k_{st}\sqrt{\left(V_D(0)\,e^{-\Theta t} + \frac{\Phi}{\Theta}\right)/\lambda_{\min}(P)} + k_{st}\,\|z_r\|_\infty \\ F_{dt}(z_{us}, z_r, t) &= c_{dt}(x_4 - \dot{z}_r) \\ &\leq c_{dt}\sqrt{\left(V_D(0)\,e^{-\Theta t} + \frac{\Phi}{\Theta}\right)/\lambda_{\min}(P)} + c_{dt}\,\|\dot{z}_r\|_\infty \end{aligned} \tag{105}$$

TABLE 1. Active suspension system parameters.

Parameter	Value	Unit
m_s	$550 \pm 100\sin(\pi t)$	kg
m_{us}	60	kg
k_s	16,000	Nm^{-1}
c_d	2300	Nsm^{-1}
k_{st}	145,000	Nm^{-1}
c_{dt}	1100	Nsm^{-1}
z_{as0}	0.18	m
z_R	0.04	m
A_{as}	0.0047	m^2
κ	1.4	-
R	287.5	$J.Kg^{-1}.K^{-1}$
T	293.15	K

Substituting (105) into (2), we can obtain relative tire force by

$$\begin{aligned} |F_{st} + F_{dt}| &\leq |F_{st}| + |F_{dt}| \\ &\leq (k_{st} + c_{dt})\sqrt{\left(V_D(0)\,e^{-\Theta t} + \frac{\Phi}{\Theta}\right)/\lambda_{\min}(P)} \\ &\quad + k_{st}\,\|z_r\|_\infty + c_{dt}\,\|\dot{z}_r\|_\infty \end{aligned} \tag{106}$$

According to (106), the relative tire force condition (11) can be ensured by selecting the design parameters ρ_1, ρ_2, P which satisfy the inequality $|F_{st} + F_{dt}| \leq (m_s + m_{us})\,g$.

Remark 8: From the above analysis, the suspension objectives of handling stability and driving safety are guaranteed by setting initial conditions and approximate design parameters. Therefore, the driving condition of the pneumatic suspension system is ensured by the mechanical structure.

IV. SIMULATION RESULTS

A. SIMULATION DEFINITION

To verify the effectiveness of the developed method, the comparative simulations are executed in comparison with passive suspension and traditional backstepping. The results of RSD and RTF parameters are compared to analyze the handling stability and driving safety of active suspension. The main parameters of pneumatic suspension are chosen as in Table 1.

To simulate the excitation of road disturbance, the sin road profile is used for the simulation studies with amplitude 0.01 m and frequency 0.5 Hz as $z_r = 0.01\sin(\pi t)$. The system is defined by these initial conditions with $x_1(0) = 0.02$, $x_2(0) = x_3(0) = x_4(0) = 0$, $x_5(0) = 1.0\times10^5\,(Pa)$. The PPF boundary is selected by $\delta_0 = 0.03$, $\delta_\infty = 0.005$, $\phi = 2$ and the control parameters are given in Table 2.

B. SIMULATION RESULTS

The simulation results of sprung mass displacement and acceleration, relative suspension deflection, relative tire

TABLE 2. Control parameters.

Control	Parameters
Backstepping	$k_1 = 5, k_2 = 5, k_3 = 10$
Proposed	$k_1 = 5\, k_2 = 5, k_3 = 10$
	$\beta_2 = 10, \beta_3 = 10, \beta_F = 10$
	$\varsigma_2 = 5, \varsigma_3 = 5, \varsigma_F = 5$
	$\rho_m = 200, \tau_m = 1$

force, and control signals of passive, traditional backstepping, and proposed control are shown in Fig. 3 - 6. The proposed scheme can improve passenger comfort by reducing the sprung mass displacement and acceleration as shown in Fig. 2 – 3. With the PPF constraint, the tracking error of vertical displacement is kept inside the predefined boundary. Although traditional backstepping can reduce the amplitude of sprung mass displacement, the output performance cannot satisfy the requirement of output constraint. Furthermore, the objectives of analyzing the handling stability and driving safety are enhanced by the proposed control because the RSD and RTF parameters are guaranteed in Fig. 4 – 5. The control signal of the proposed scheme with the CFC technique is shown in Fig. 6. Although the proposed method requires a large control signal at the beginning to guarantee the speed convergence of tracking error, its required signal will be smaller as soon as the constraint boundary is satisfied.

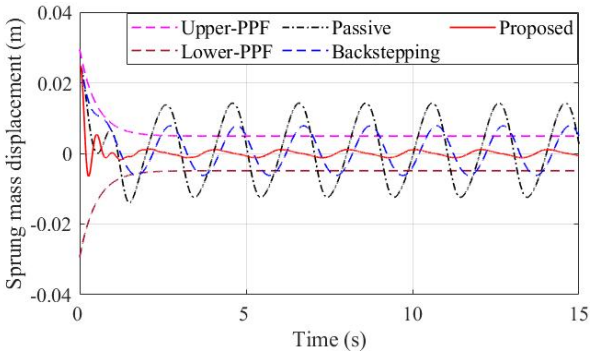

FIGURE 2. Simulation result of sprung mass displacement.

V. EXPERIMENTAL RESULTS

A. EXPERIMENTAL PLATFORM

The quarter car test bench for active suspension with a pneumatic spring is designed to verify the effectiveness of the proposed controller, which is displayed in Fig. 7. Due to the limitation of mechanical structure, the main parameters are chosen in accordance with the platform design. There are three separate plates that are used to represent the chassis, tire, and road profile, and they are connected by mechanical and pneumatic springs. The chassis is denoted by the top plate and it is supported by a pneumatic spring and two mechanical

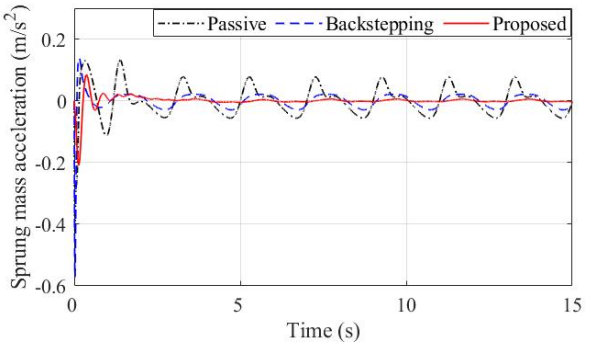

FIGURE 3. Vertical acceleration responses of sprung mass.

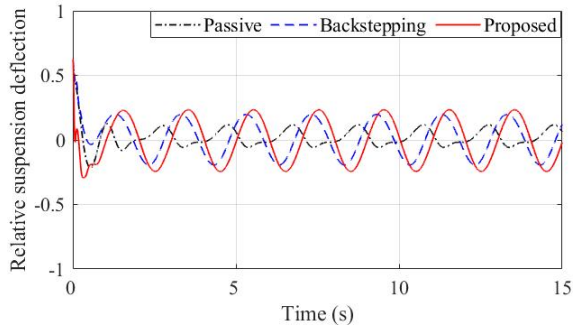

FIGURE 4. Simulation result of relative suspension deflection.

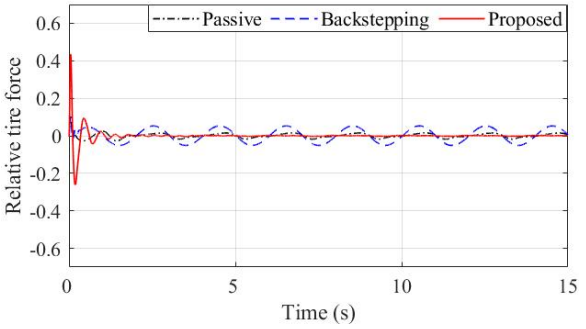

FIGURE 5. Simulation result of relative tire force.

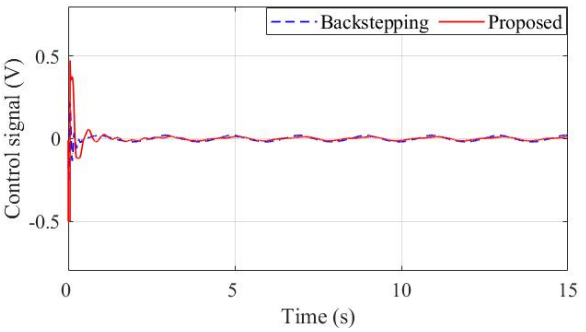

FIGURE 6. Simulation result of control signal (V).

springs. The middle plate is used to simulate the motion of tire and structure assembly. The road profile is simulated by the motion of the bottom plate, which is driven by the servo motor

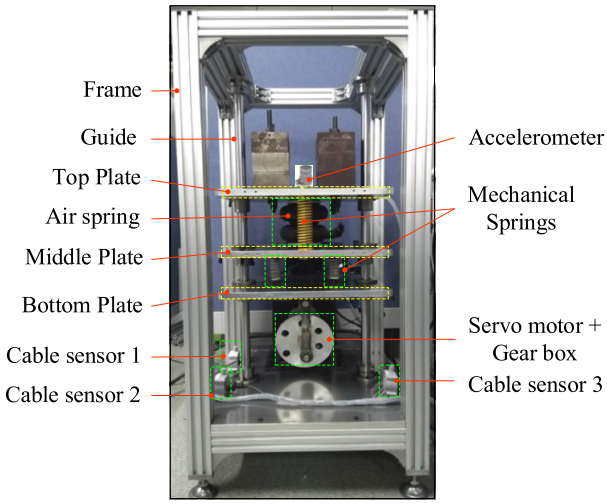

FIGURE 7. Platform of pneumatic active suspension.

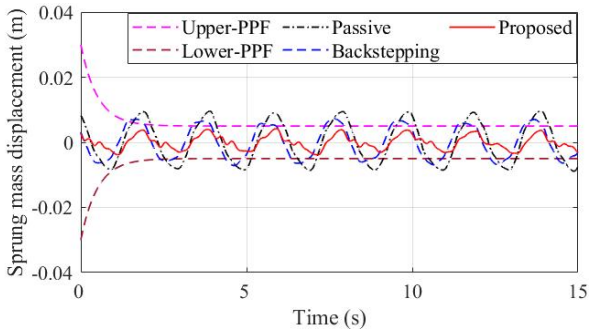

FIGURE 8. Experimental result of sprung mass displacement.

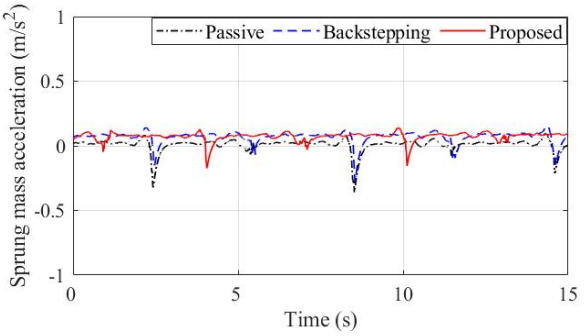

FIGURE 9. Experimental result of sprung mass acceleration.

to create various road conditions. The stiffness coefficient of a tire is represented by two mechanical springs. Besides, three cable sensors are used to measure the position of the three plates. A piezoelectric accelerometer is employed to determine the acceleration of the chassis. A PCI card is used to record and send the control signal between the computer and the proportional pneumatic valve.

B. EXPERIMENTAL RESULTS

The experiment results of the pneumatic active suspension carried on the test bench are displayed in Fig. 8 – 12. We can

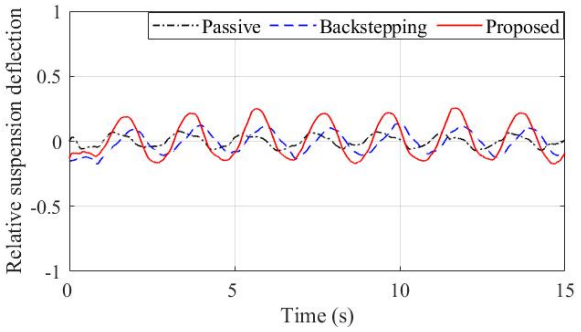

FIGURE 10. Experimental result of relative suspension deflection.

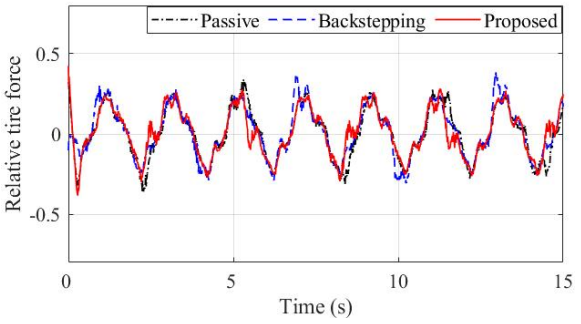

FIGURE 11. Experimental result of relative tire force.

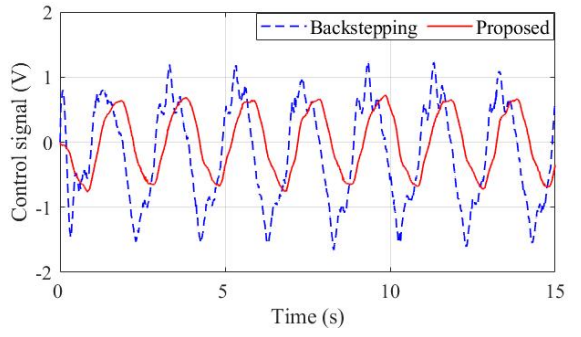

FIGURE 12. Experimental result of control signal.

see that the experimental results also demonstrate the effectiveness of the proposed control in comparison with the backstepping approach. From Fig. 8, the vertical displacement of sprung mass can be restrained within the PPF constraint of the proposed scheme. Since the active suspension enhances the ride comfort resulting in a larger suspension stroke, the RSD value of the proposed control is greater than the passive suspension and traditional backstepping. Besides, the RSD and RTF parameters are also maintained to be less than 1 to achieve the goals of handling stability and driving safety of the pneumatic active suspension. Although there are different values between the simulation and experimental results, both are able to demonstrate the efficiency of the proposed controller. Similar to the simulation results, the control signal of the proposed controller is smaller than that of the traditional backstepping technique.

VI. CONCLUSION

This article investigates an adaptive fuzzy observer fault tolerant scheme for the active suspension which considers the uncertain parameters and the failure problem of pneumatic spring. The adaptive fuzzy observer based command filtered is designed to solve the problem of actuator failures where both of loss of effectiveness model and lock-in-place model are considered. The PPF constraint is employed to restrain the sprung mass movement to get the passenger comfort while the CFC technique is proposed to avoid the explosion of complexity problem of the traditional backstepping approach. By using the fuzzy logic systems method to estimate unknown nonlinear functions and then incorporate them into the nonlinear disturbance observer, the external disturbances and unknown actuator failure coefficients are estimated. Moreover, the effectiveness of the designed controller has been verified by both simulation and experiment, which considers control objectives of the passenger comfort, driving safety, and handling stability for the active suspension system.

Further research includes the implementation of the proposed fault tolerant control design to stabilize the full-car pneumatic active suspension.

REFERENCES

[1] Y. Zhang and L. Liu, "Adaptive fault tolerant control of active suspension systems with time-varying displacement and velocity constraints," *IEEE Access*, vol. 8, pp. 10847–10856, 2020, doi: 10.1109/access.2020.2964722.

[2] S. Basaran and M. Basaran, "Vibration control of truck cabins with the adaptive vectorial backstepping design of electromagnetic active suspension system," *IEEE Access*, vol. 8, pp. 173056–173067, 2020, doi: 10.1109/access.2020.3025357.

[3] Y.-J. Liu, Q. Zeng, L. Liu, and S. Tong, "An adaptive neural network controller for active suspension systems with hydraulic actuator," *IEEE Trans. Syst., Man, Cybern. Syst.*, vol. 50, no. 12, pp. 5351–5360, Dec. 2020, doi: 10.1109/tsmc.2018.2875187.

[4] H.-Y. Chen and J.-W. Liang, "Adaptive wavelet neural network controller for active suppression control of a diaphragm-type pneumatic vibration isolator," *Int. J. Control, Autom. Syst.*, vol. 15, no. 3, pp. 1456–1465, Jun. 2017, doi: 10.1007/s12555-014-0428-2.

[5] H. Zhu, J. Yang, Y. Zhang, and X. Feng, "A novel air spring dynamic model with pneumatic thermodynamics, effective friction and viscoelastic damping," *J. Sound Vib.*, vol. 408, pp. 87–104, Nov. 2017, doi: 10.1016/j.jsv.2017.07.015.

[6] X. Ma, P. K. Wong, J. Zhao, J.-H. Zhong, H. Ying, and X. Xu, "Design and testing of a nonlinear model predictive controller for ride height control of automotive semi-Active air suspension systems," *IEEE Access*, vol. 6, pp. 63777–63793, 2018, doi: 10.1109/ACCESS.2018.2876496.

[7] J. Na, Y. Huang, X. Wu, G. Gao, G. Herrmann, and J. Z. Jiang, "Active adaptive estimation and control for vehicle suspensions with prescribed performance," *IEEE Trans. Control Syst. Technol.*, vol. 26, no. 6, pp. 2063–2077, Nov. 2018, doi: 10.1109/TCST.2017.2746060.

[8] G. Yan, M. Fang, and J. Xu, "Analysis and experiment of time-delayed optimal control for vehicle suspension system," *J. Sound Vib.*, vol. 446, pp. 144–158, Apr. 2019, doi: 10.1016/j.jsv.2019.01.015.

[9] H. Pang, Y. Shang, and P. Wang, "Design of a sliding mode observer-based fault tolerant controller for automobile active suspensions with parameter uncertainties and sensor faults," *IEEE Access*, vol. 8, pp. 186963–186975, 2020, doi: 10.1109/access.2020.3029815.

[10] B. Lin and X. Su, "Fault-tolerant controller design for active suspension system with proportional differential sliding mode observer," *Int. J. Control, Autom. Syst.*, vol. 17, no. 7, pp. 1751–1761, Jul. 2019, doi: 10.1007/s12555-018-0630-8.

[11] H. Pang, X. Zhang, and Z. Xu, "Adaptive backstepping-based tracking control design for nonlinear active suspension system with parameter uncertainties and safety constraints," *ISA Trans.*, vol. 88, pp. 23–36, May 2019, doi: 10.1016/j.isatra.2018.11.047.

[12] H. Nazemian and M. Masih-Tehrani, "Development of an optimized game controller for energy saving in a novel interconnected air suspension system," *Proc. Inst. Mech. Eng., D, J. Automobile Eng.*, vol. 234, no. 13, pp. 3068–3080, Nov. 2020, doi: 10.1177/0954407020927147.

[13] H. Kim and H. Lee, "Height and leveling control of automotive air suspension system using sliding mode approach," *IEEE Trans. Veh. Technol.*, vol. 60, no. 5, pp. 2027–2041, Jun. 2011, doi: 10.1109/TVT.2011.2138730.

[14] Y.-J. Liang, N. Li, D.-X. Gao, and Z.-S. Wang, "Optimal vibration control for nonlinear systems of tracked vehicle half-car suspensions," *Int. J. Control, Automat. Syst.*, vol. 15, no. 4, pp. 1675–1683, 2017, doi: 10.1007/s12555-015-0447-7.

[15] B. Rui, "Nonlinear adaptive sliding-mode control of the electronically controlled air suspension system," *Int. J. Adv. Robot. Syst.*, vol. 16, no. 5, Sep. 2019, Art. no. 172988141988152, doi: 10.1177/1729881419881527.

[16] R. Zhao, W. Xie, P. K. Wong, D. Cabecinhas, and C. Silvestre, "Robust ride height control for active air suspension systems with multiple unmodeled dynamics and parametric uncertainties," *IEEE Access*, vol. 7, pp. 59185–59199, 2019, doi: 10.1109/ACCESS.2019.2913451.

[17] C. M. Ho, D. T. Tran, C. H. Nguyen, and K. K. Ahn, "Adaptive neural command filtered control for pneumatic active suspension with prescribed performance and input saturation," *IEEE Access*, vol. 9, pp. 56855–56868, 2021, doi: 10.1109/access.2021.3071322.

[18] W. Sun, H. Gao, and O. Kaynak, "Adaptive backstepping control for active suspension systems with hard constraints," *IEEE/ASME Trans. Mechatronics*, vol. 18, no. 3, pp. 1072–1079, Jun. 2013, doi: 10.1109/tmech.2012.2204765.

[19] S. Zhang, W.-Y. Cui, and F. E. Alsaadi, "Adaptive backstepping control design for uncertain non-smooth strictfeedback nonlinear systems with time-varying delays," *Int. J. Control, Autom. Syst.*, vol. 17, no. 9, pp. 2220–2233, 2019, doi: 10.1007/s12555-019-0046-0.

[20] C. P. Bechlioulis and G. A. Rovithakis, "Robust adaptive control of feedback linearizable MIMO nonlinear systems with prescribed performance," *IEEE Trans. Autom. Control*, vol. 53, no. 9, pp. 2090–2099, Oct. 2008,doi: 10.1109/tac.2008.929402.

[21] A. K. Kostarigka and G. A. Rovithakis, "Adaptive dynamic output feedback neural network control of uncertain MIMO nonlinear systems with prescribed performance," *IEEE Trans. Neural Netw. Learn. Syst.*, vol. 23, no. 1, pp. 49–138, Jan. 2012, doi: 10.1109/TNNLS.2011.2178448.

[22] R. M. Sanner and J.-J.-E. Slotine, "Gaussian networks for direct adaptive control," *IEEE Trans. Neural Netw.*, vol. 3, no. 6, pp. 837–863, 1992.

[23] S. Wen, Z. Q. M. Chen, X. Yu, Z. Zeng, and T. Huang, "Fuzzy control for uncertain vehicle active suspension systems via dynamic sliding-mode approach," *IEEE Trans. Syst., Man, Cybern., Syst.*, vol. 47, no. 1, pp. 24–32, Jan. 2017, doi: 10.1109/tsmc.2016.2564930.

[24] X. Min, Y. Li, and S. Tong, "Adaptive fuzzy output feedback inverse optimal control for vehicle active suspension systems," *Neurocomputing*, vol. 403, pp. 257–267, Aug. 2020, doi: 10.1016/j.neucom.2020.04.096.

[25] X. Min, Y. Li, and S. Tong, "Adaptive fuzzy optimal control for a class of active suspension systems with full-state constraints," *IET Intell. Transp. Syst.*, vol. 14, no. 5, pp. 371–381, May 2020, doi: 10.1049/iet-its.2019.0187.

[26] J. Na, Y. Huang, X. Wu, S. Su, and G. Li, "Adaptive finite-time fuzzy control of nonlinear active suspension systems with input delay," *IEEE Trans. Cybern.*, vol. 50, no. 6, pp. 2639–2650, Jun. 2020, doi: 10.1109/TCYB.2019.2894724.

[27] Y.-J. Liu, Q. Zeng, S. Tong, C. L. P. Chen, and L. Liu, "Adaptive neural network control for active suspension systems with time-varying vertical displacement and speed constraints," *IEEE Trans. Ind. Electron.*, vol. 66, no. 12, pp. 9458–9466, Dec. 2019, doi: 10.1109/TIE.2019.2893847.

[28] H. Li, Z. Zhang, H. Yan, and X. Xie, "Adaptive event-triggered fuzzy control for uncertain active suspension systems," *IEEE Trans. Cybern.*, vol. 49, no. 12, pp. 4388–4397, Dec. 2019, doi: 10.1109/TCYB.2018.2864776.

[29] D. Ning, S. Sun, F. Zhang, H. Du, W. Li, and B. Zhang, "Disturbance observer based takagi-sugeno fuzzy control for an active seat suspension," *Mech. Syst. Signal Process.*, vol. 93, pp. 515–530, Sep. 2017, doi: 10.1016/j.ymssp.2017.02.029.

[30] S. Liu, B. Jiang, Z. Mao, and S. X. Ding, "Adaptive backstepping based fault-tolerant control for high-speed trains with actuator faults," *Int. J. Control, Autom. Syst.*, vol. 17, no. 6, pp. 1408–1420, Jun. 2019, doi: 10.1007/s12555-018-0703-8.

[31] R. Ji, J. Ma, D. Li, and S. S. Ge, "Finite-time adaptive output feedback control for MIMO nonlinear systems with actuator faults and saturations," *IEEE Trans. Fuzzy Syst.*, vol. 29, no. 8, pp. 2256–2270, Aug. 2021, doi: 10.1109/tfuzz.2020.2996709.

[32] J. A. Farrell, M. Polycarpou, M. Sharma, and W. Dong, "Command filtered backstepping," *IEEE Trans. Autom. Control*, vol. 54, no. 6, pp. 1391–1395, Jun. 2009, doi: 10.1109/tac.2009.2015562.

[33] J. Qiu, K. Sun, I. J. Rudas, and H. Gao, "Command filter-based adaptive NN control for MIMO nonlinear systems with full-state constraints and actuator hysteresis," *IEEE Trans. Cybern.*, vol. 50, no. 7, pp. 2905–2915, Jul. 2020, doi: 10.1109/TCYB.2019.2944761.

[34] M. Dong, G. Tao, L. Wen, and B. Jiang, "Adaptive sensor fault detection for rail vehicle suspension systems," *IEEE Trans. Veh. Technol.*, vol. 68, no. 8, pp. 7552–7565, Aug. 2019, doi: 10.1109/tvt.2019.2926225.

[35] Z. Liu, J. Liang, Z. Zhao, M. O. Efe, and K.-S. Hong, "Adaptive fault-tolerant control of a probe-and-drogue refueling hose under varying length and constrained output," *IEEE Trans. Control Syst. Technol.*, early access, May 25, 2021, doi: 10.1109/tcst.2021.3079275.

[36] Y. Nai, Q. Yang, and Z. Zhang, "Adaptive neural output feedback compensation control for intermittent actuator faults using command-filtered backstepping," *IEEE Trans. Neural Netw. Learn. Syst.*, vol. 31, no. 9, pp. 3497–3511, Sep. 2020, doi: 10.1109/TNNLS.2019.2944897.

[37] Z. Zhao, Z. Liu, W. He, K.-S. Hong, and H.-X. Li, "Boundary adaptive fault-tolerant control for a flexible Timoshenko arm with backlash-like hysteresis," *Automatica*, vol. 130, Aug. 2021, Art. no. 109690, doi: 10.1016/j.automatica.2021.109690.

[38] W. Sun, H. Gao, and O. Kaynak, "Vibration isolation for active suspensions with performance constraints and actuator saturation," *IEEE/ASME Trans. Mechatronics*, vol. 20, no. 2, pp. 675–683, Apr. 2015, doi: 10.1109/tmech.2014.2319355.

[39] Y.-H. Jing and G.-H. Yang, "Fuzzy adaptive fault-tolerant control for uncertain nonlinear systems with unknown dead-zone and unmodeled dynamics," *IEEE Trans. Fuzzy Syst.*, vol. 27, no. 12, pp. 2265–2278, Dec. 2019, doi: 10.1109/tfuzz.2019.2896844.

[40] B. Liu, M. Saif, and H. Fan, "Adaptive fault tolerant control of a half-car active suspension systems subject to random actuator failures," *IEEE/ASME Trans. Mechatronics*, vol. 21, no. 6, pp. 2847–2857, Dec. 2016, doi: 10.1109/tmech.2016.2587159.

[41] Y. Ren, P. Zhu, Z. Zhao, J. Yang, and T. Zou, "Adaptive fault-tolerant boundary control for a flexible string with unknown dead zone and actuator fault," *IEEE Trans. Cybern.*, early access, Jan. 21, 2021, doi: 10.1109/TCYB.2020.3044144.

[42] Y.-J. Liu, Q. Zeng, S. Tong, C. L. P. Chen, and L. Liu, "Actuator failure compensation-based adaptive control of active suspension systems with prescribed performance," *IEEE Trans. Ind. Electron.*, vol. 67, no. 8, pp. 7044–7053, Aug. 2020, doi: 10.1109/tie.2019.2937037.

[43] Z. Zhao, Y. Ren, C. Mu, T. Zou, and K.-S. Hong, "Adaptive neural-network-based fault-tolerant control for a flexible string with composite disturbance observer and input constraints," *IEEE Trans. Cybern.*, early access, Jul. 7, 2021, doi: 10.1109/TCYB.2021.3090417.

[44] Y.-H. Jing and G.-H. Yang, "Adaptive fuzzy output feedback fault-tolerant compensation for uncertain nonlinear systems with infinite number of time-varying actuator failures and full-state constraints," *IEEE Trans. Cybern.*, vol. 51, no. 2, pp. 568–578, Feb. 2021, doi: 10.1109/TCYB.2019.2904768.

[45] R. Wang, H. Jing, H. R. Karimi, and N. Chen, "Robust fault-tolerant H_∞ control of active suspension systems with finite-frequency constraint," *Mech. Syst. Signal Process.*, vols. 62–63, pp. 341–355, Oct. 2015, doi: 10.1016/j.ymssp.2015.01.015.

[46] A. Bounemeur, M. Chemachema, and N. Essounbouli, "Indirect adaptive fuzzy fault-tolerant tracking control for MIMO nonlinear systems with actuator and sensor failures," *ISA Trans.*, vol. 79, pp. 45–61, Aug. 2018, doi: 10.1016/j.isatra.2018.04.014.

[47] X. Yu, H. Pan, W. Sun, and H. Gao, "Reliable control for a class of nonlinear time-delay systems against actuator faults with application to suspension control," *IEEE/ASME Trans. Mechatronics*, vol. 24, no. 6, pp. 2498–2507, Dec. 2019, doi: 10.1109/TMECH.2019.2948477.

[48] J. J. Rath, M. Defoort, C. Sentouh, H. R. Karimi, and K. C. Veluvolu, "Output-constrained robust sliding mode based nonlinear active suspension control," *IEEE Trans. Ind. Electron.*, vol. 67, no. 12, pp. 10652–10662, Dec. 2020, doi: 10.1109/tie.2020.2978693.

[49] C. Kim and P. I. Ro, "A sliding mode controller for vehicle active suspension systems with non-linearities," *Proc. Inst. Mech. Eng., D, J. Auto. Eng.*, vol. 212, no. 2, pp. 79–92, 1998.

[50] F. de Melo, A. Pereira, and A. Morais, "The simulation of an automotive air spring suspension using a pseudo-dynamic procedure," *Appl. Sci.*, vol. 8, no. 7, pp. 1049–1068, 2018, doi: 10.3390/app8071049.

[51] L. Wang, M. V. Basin, H. Li, and R. Lu, "Observer-based composite adaptive fuzzy control for nonstrict-feedback systems with actuator failures," *IEEE Trans. Fuzzy Syst.*, vol. 26, no. 4, pp. 2336–2347, Aug. 2018, doi: 10.1109/tfuzz.2017.2774185.

[52] L.-X. Wang and J. M. Mendel, "Fuzzy basis functions, universal approximation, and orthogonal least-squares learning," *IEEE Trans. Neural Netw.*, vol. 3, no. 5, pp. 807–814, 1992, doi: 10.1109/72.159070.

[53] L.-X. Wang, "Stable adaptive fuzzy control of nonlinear systems," *IEEE Trans. Fuzzy Syst.*, vol. 1, no. 2, pp. 146–155, May 1993, doi: 10.1109/91.227383.

[54] W. Dong, J. A. Farrell, M. M. Polycarpou, V. Djapic, and M. Sharma, "Command filtered adaptive backstepping," *IEEE Trans. Control Syst. Technol.*, vol. 20, no. 3, pp. 566–580, May 2012, doi: 10.1109/tcst.2011.2121907.

[55] Y. Huang, J. Na, X. Wu, X. Liu, and Y. Guo, "Adaptive control of nonlinear uncertain active suspension systems with prescribed performance," *ISA Trans.*, vol. 54, pp. 145–155, Jan. 2015, doi: 10.1016/j.isatra.2014.05.025.

CONG MINH HO received the B.S. degree from the Department of Mechanical Engineering, Ho Chi Minh City University of Technology, Ho Chi Minh City, Vietnam, in 2008, and the M.S. degree from the Department of Mechanical Engineering, Ho Chi Minh City University of Technology and Education, in 2018. He is currently pursuing the Ph.D. degree with the School of Mechanical Engineering, University of Ulsan, Ulsan, South Korea.

His research interests include adaptive control, fluid power control, and active suspension systems.

KYOUNG KWAN AHN (Senior Member, IEEE) received the B.S. degree from the Department of Mechanical Engineering, Seoul National University, in 1990, the M.Sc. degree in mechanical engineering from Korea Advanced Institute of Science and Technology, in 1992, and the Ph.D. degree from Tokyo Institute of Technology, in 1999.

He is currently a Professor with the School of Mechanical Engineering, University of Ulsan, Ulsan, South Korea. His research interests include design and control of smart actuator using the smart material, fluid power control and active damping control, and renewable energy. He is an Editor of *IJCAS* and an Editorial Board Member of *Renewable Energy*, *Actuators*, and *Journal of Engineering*.